International Journal of Engineering Research and Development
e- ISSN: 2278-067X, p-ISSN: 2278-800X, www.ijerd.com
Volume 22, Issue 3 (March 2026), PP 204-220

Depletion-Driven Geomechanical Feedback and Post-Fracture Productivity Decline in Unconventional Reservoirs: An Integrated Framework Coupling Stress Reorientation, Proppant Embedment, And Dynamic Conductivity Loss

Engr. Dr. Ekeinde Evelyn Bose
Department of Petroleum and Gas Engineering, Federal University Otuoke, Bayelsa State,

Abstract
Unconventional and mature reservoir development continues to be based on hydraulic fracturing, but post-treatment production never meets the original predictions because of unpredicted geomechanical feedbacks caused by reservoir depletion. This review article is a compilation of a decade of rock mechanics advances (20152024) to systematically investigate how stress reorientation caused by depletion, the proppant embedment and the systematic loss of dynamic fracture conductivity are all contributing factors to the long-term well productivity in depleted unconventional reservoirs. Critical evaluation of peer-reviewed literature indicates a current research gap: these mutually reinforcing phenomena in geomechanics have been studied in isolation by the academic community and industry community workers alike, leading to a systematic over-prediction of productivity indices (PI) with no less than a 50 percent error in the sensible applications of mature field processes. Poroelastic depletion with subsequent minimum horizontal stress (Δσhmin) of over 30 says azimuthal shifts in the geometry of future fracture invasion of subsequent fracture campaigns in infill and refracturing. Simultaneously, undergoing high closure stress especially in clay shale with low values of Youngs modulus of less than 5Gpa proppant embedment can lead to a reduction in effective fracture aperture by 40-70 percent in rapid conductivity deterioration faster than that indicated by precise laboratory phenomena. This review suggests a radical change in thinking to not static fracture design but time varying geomechanical hydrodynamic paradigm which integrates poroelastic development of stresses with nonlinear embedment plasticity and dynamic flow modelling. The integrated models have demonstrated by field cases study in the Permian Basin, Eagle Ford and Sichuan Basin that the PI prediction error of 50 and less have been reduced to less than 15 percent which is a paradigm shift in operation decision making. The synthesis concludes that machine learning augmentation bears the most crucial facilitator of executing the diligence in-between bridging the computational hindrances that have impeded thus far total field Tie away made the physics associations a relic of the past.

Keywords: *rock mechanics, hydraulic fracturing, stress reorientation, proppant embedment, fracture conductivity, productivity index, reservoir depletion, poroelasticity, unconventional reservoirs.*

Date of Submission: 08-03-2026 Date of acceptance: 20-03-2026

I. Introduction

The application of hydraulic fracturing has essentially revolutionized the recovery of hydrocarbons in low-permeability unconventional reservoirs, but field performance records have continued to show that a significant percentage of stimulated wells do not achieve the initial production projections. Incompletion designs that are suboptimal may lead to poorly performing wells: fractures can interfere with the fractures during the process of multistage stimulation, which in turn implies that not all the perforations can be fractured, and only a fraction of the fractures ultimately give significant production contributions (Lin et al., 2022), and unruly well behaviour only worsens the situation with forecasting production and reserve (Weijermars, 2023). The results of this systematic underperformance in economic terms incline greatly: resource estimates, which are not aligned, sub-optimal capital placement and a fastening environmental rest upon per unit energy created. There are many engineering factors to play up to this mismatch, although it is convergent evidence that identifies depletion-stimulated geomechanical feedbacks to prevail over fracture network development, and the progressive decrease in fracture conductivity. Changes in the in-situ stress field due to depletion-induced stress cause re-orientation of the outlying major stresses that directly controls the fractures propagation in infill wells (Zhang et al., 2022).

The traditional practice of fracture design is mostly based on the application of the static geomechanical models, in which in-situ stress states are assumed to be invariant, and proppant behavior is assumed to be idealized. This is a computationally convenient assumption but is fundamentally inconsistent with the physics of the

reservoirs in mature and densely drilled fields where parent-child well interaction, stress reorientation caused by depletion and proppant degrading over time act as a coupled time evolving system. Even within wells that are completed using similar fracture treatment designs in the same reservoir, there is an extreme spread in the production results, which cannot be attributed to completion geometry itself and which is indicative of the insufficiency of various systems of static modeling that are unable to include the development in situ with time (Tugan & Weijermars, 2022). Moreover, as many hydraulic fractures grow in parallel, the non-uniform division of the fluids and the processes of stress-interference-based non-planar fracture geometries become dynamic effects that are completely not considered in the framework of invariant-stress design (Lecampion & Desroches, 2015). The inability to model the unexpected couplings is associated with fractures propagating unexpectedly, loss of conductivity particularly at high distances, premature well depletion, and economic and environmental expenses that could easily be reduced through better modeling practice.

The unaddressed and long-standing research gap that can be found in this review is the lack of a single, predictive system to integrate depletion-induced stress re-orientation, proppant embedment and subsequent conductivity loss and post-fracture productivity index (PI) modeling into a unified, time-changing, coupled system. Although seen independently, significant progress in each of these areas has occurred within the last decade, the interactions between them are concurrently and have not been well quantified in the extant literature. In the wide basins, deep and ultra-deep shale gas wells have shown a high level of variation in production and have not reached the desired level where the hydraulic fracturing designs mainly used the traditional technique based on the experience of the shallow reservoirs (Zhao et al., 2025). This knowledge gap is an increasingly costly operating liability as operators grow their operations in depleted zones across key unconventional assets (where traditional fracturing operations combined with depletion are concomitant, altering a stress state that controls new fracture paths (Lin et al., 2022)) to refracturing operations and infill well initiatives.

The point that is furthered here is that the next step toward reservoir stimulation is not new fracturing fluids or proppant chemistries per se but an adaptive geomechanical modelling process that brings to bear the dynamically coupled rock fluid proppant system through the useful productive life of the fracturing well.

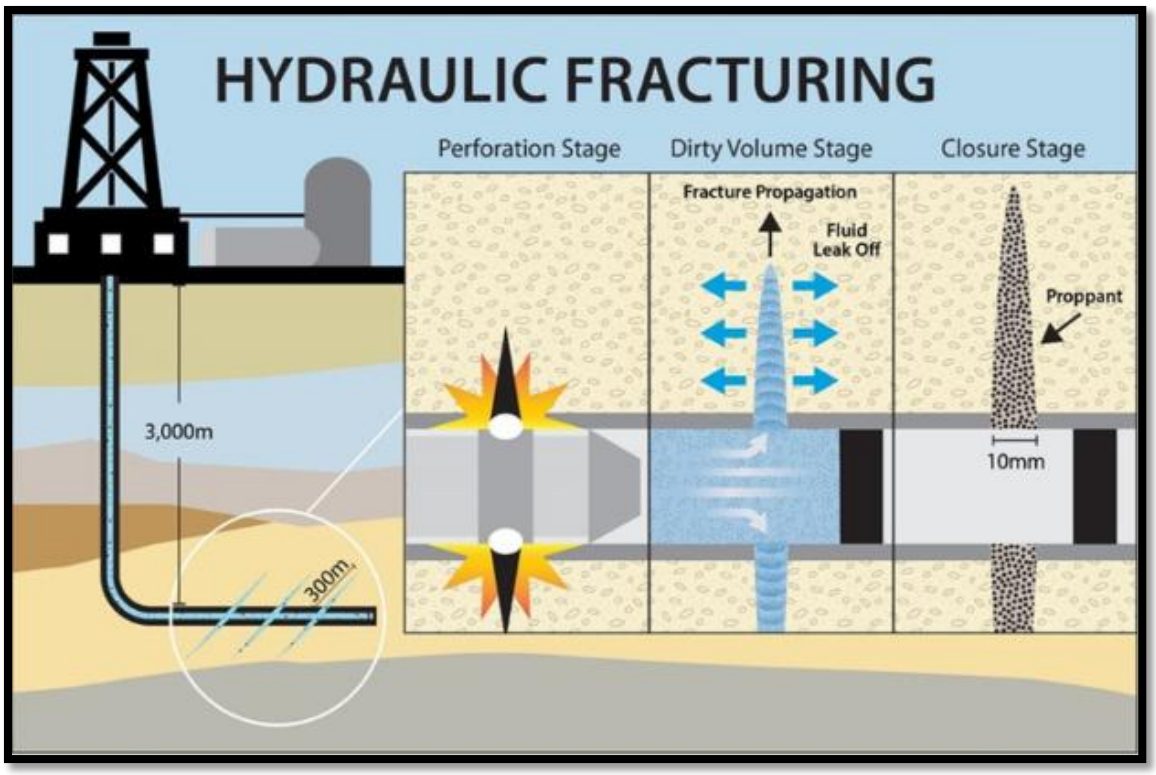

Figure 1. Schematic sketch of the hydraulic fracturing process showing three stages involved in the operation which can be applied in the present review: perforation, fracture propagation (leak-off of fluids, fracture expansion at an approximate depth of 3,000 m), and closure (proppant packing at a scale of approximately 10 mm ensuring the conductivity). (Kwon Research Group. 2026)

Depletion-Induced Stress Reorientation: Mechanisms and Quantification

The in-situ stress tensor defined by the vertical stress (σv) and the two principal horizontal stresses (σHmax and σhmin) governs hydraulic fracture propagation direction, geometry, and containment. In the normal

faulting regime characteristic of most North American unconventional basins, fractures propagate as vertical planes perpendicular to σhmin. This is not a constant state of stress. Reduction in pore pressure (Pp) during production causes poroelastic deformation, which redistributes stress in an non-uniform way with respect to the drainage geometry, rock elastic properties and heterogeneity of the reservoirs. Field data, the Ekofisk Field confirmed that the effective stresses in a linearly increasing manner with a pore pressure drawdown, but at significantly different rates between the horizontal and vertical components, that is, showing that depletion does not uniformly compress the stress matrix but reshapes it in a differently forming way (Teufel et al., 1991).

This phenomenon stress reorientation caused by depletion alters the magnitude and the azimuth of σhmin, and can have a potentially transformative implication on any subsequent fracture treatment which is administered to the reservoir. The basic process is the poroelastic coupling where the shrinkage of pore pressure elevates effective stress. Since the depletion process is spatially heterogeneous and non-uniformly distributed in nature, due to concentration along major cracks and hydraulic fracture systems, the existence of dissimilar stress gradients in the vicinity of permeable backgrounds and fractures of hydraulic fractures cause the occurrence of stress gradients that are capable of altering the principal stress

directions by measurable degrees, and this occurs even when the fractures are depleted (Jin & Zoback, 2019).

Major North American shale plays have since been modeled and studied in the field and their heterogeneity of these stress rotations is experimentally verified to form so-called stress shadow near infill wells that either enhance or retard the propagation of fractures in directions inconsistent with what a system of static models can predict predictably. A reduced in-situ differential stress creates a greater stress reorientation caused by depletion and generates longitudinal fractures along infill wells, which significantly decrease stimulated reservoir volume and initial well performance; a larger differential stress creates a lesser reorientation but high chances of fractures propagating directly parallel existing fractures, creating damaging frac hits, thus impairing production in parent and child wells (Guo et al., 2019). Such asymmetrical propagation to the depleted side of the reservoir which child fractures can intersect pre-existing hydraulic fractures or the pre-existing wellbore is one of the key sources of production interference and a faster rate of decline in both wells (Lecampion & Desroches, 2021). Zhang et al. (2022) further confirmed numerically that depletion-induced principal stress reorientation directly governs infill well fracture propagation trajectories, underscoring the inadequacy of static stress assumptions in densely developed unconventional plays.

Poroelastic Stress Change: Governing Equation

The poroelastic relationship that acts as the governing equation in change in stress because of a decrease in pore pressure is put form in Biot poroelastic formulation. The equation change in total components of stress of an isotropic, homogeneous, porous medium as a result of change in pore pressure is:

$$\Delta\sigma_{ij} = \alpha \cdot \Delta P_p \cdot \delta_{ij}$$

Equation 1: Poroelastic Stress Change (Detournay & Cheng, 2016)

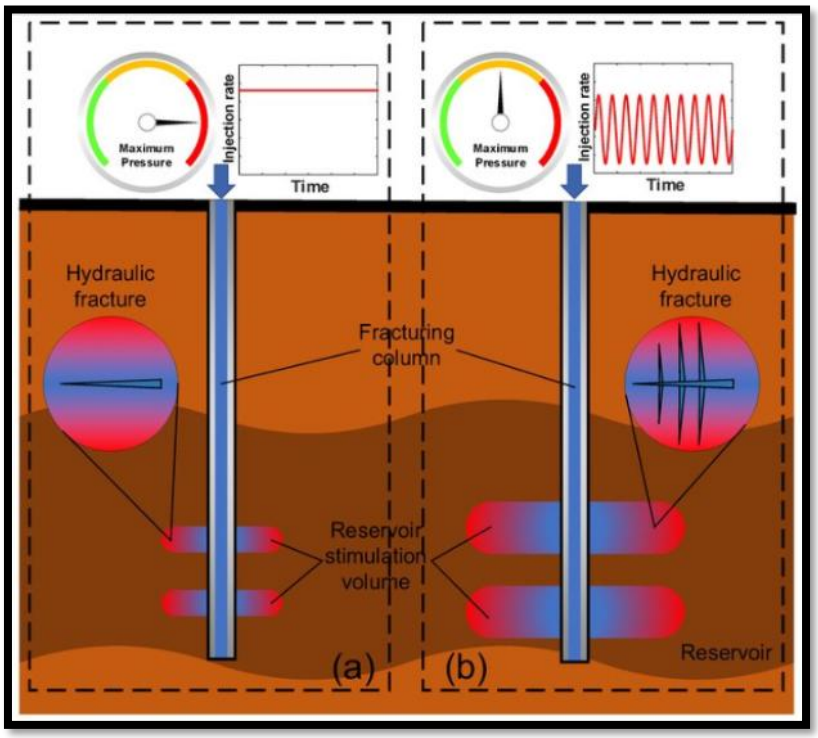

*Figure 2. Fracture-stress rotation Two-panel diagram to show stress rotation as a result of depletion. The first uniform stress field of two intended wells with linear hydraulic fracture geometry is represented in panel (A). The post-production reorientation condition is depicted at the panel (B) resulting in an asymmetric curving of the child-well fracture towards the parent wellbore. (Zhang et al., 2024)*In this case, α is the poroelastic coefficient of Biot (the coefficient being equal to 0.6-0.9 to represent most shale formations), 0pp is the change of pore pressure by the production and 0 i 0 know g an (Detournay and Cheng, 2016). It is a simplified expression that assumes isotropic environments, and one-dimensional depletion but actual reservoirs are anisotropic elastic media, have complicated drainage morphology, and have non-uniform lithologic sequences, which require three-dimensional poroelastic modeling.

Advanced Numerical Modeling of Stress Reorientation

Simulations using three-dimensional finite elements (FEM) and discrete fracture network (DFN) have contributed significantly to the quantitative knowledge on stress reorientation. Poroelastic FEMs with complete coupling reveal that the redistribution of stress in and around depleting wells is axisymmetric and proportional not only to the magnitude of depletion except alone, but also highly determined by the layering of formations, natural fracture networks, and mechanical dissimilarities among lithologic units. A 3D FEM reservoir-geomechanics analysis of Eagle Ford Shale showed that the response of stress reorientation caused by parent well depletion appears within a year of production and can exhibit a complete transformation to a 90° principal stress reversal within a matter of months later, with bottomhole pressure, the reversal between differential stress and parent well fracture geometry all found noteworthy agents of this transformation (Guo et al., 2018). Subsequent coupled reservoir/geomechanics/fracturing simulations verified that stirred by low differential stress conditions, stress-reorientation caused by depletion creates longitudinal fractures along infill wells, which severely depletes stimulated reservoir volume and initial well performance whereas under high differential stress fractures preferentially propagate toward existing fractures, creating damaging frac hits that hamper production of parent and child wells (Guo et al., 2019). The outcome of these modelling studies indicate that fracture deflection, the removal of complexity, and inter-well communication in the stimulation treatments are foreseeable events due to neglect in depletion-state stress field consideration in the design of fractures.

Its practical application is saline: the design of fractures in wells of infill and refracturing campaigns has to be performed with a dynamic model of maintaining stress changed to the present area of the reservoir depleted state. Field application in the Midland Basin confirms that depletion causes asymmetric fracture growth toward depleted regions with direct negative consequences for infill well production capacity, and that modeling-guided determination of optimal well spacing and treatment design under these depletion conditions is necessary to minimize frac hits and reduce unnecessary completion costs (Levon et al., 2021). Integrated geomechanical modeling further demonstrates that the degree of parent–child fracture interference is not static: elongating parent well production time prior to infill drilling progressively aggravates asymmetric fracture growth, underscoring

that both timing and spacing decisions must be anchored to a continuously updated depletion model (Pei et al., 2023).

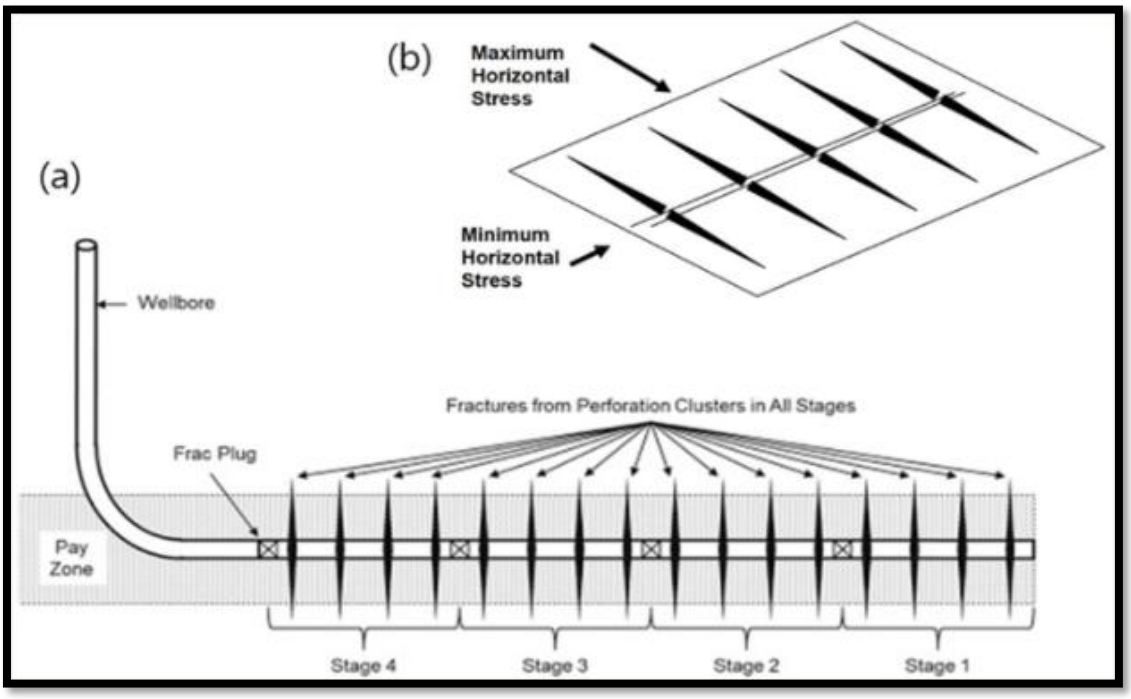

Figure 3. Geomechanical illustration of stress reversals near hydraulically fractured wells explained through poroelasticity. Panel (a) depicts the multi-stage fracturing geometry in a horizontal wellbore (Stages 1–4) with fractures initiating at perforation clusters across the pay zone. Panel (b) shows the 3D stress field configuration with maximum and minimum horizontal stress (σHmax and σhmin) orientations. **(Weijermars & Wang, 2021)**

Proppant Embedment and Dynamic Fracture Conductivity Loss

Fracture conductivity (kfw) is the product of fracture permeability and fracture width, and it represents the primary pathway for hydrocarbon flow from the reservoir matrix to the wellbore. The maintenance of adequate conductivity over the productive life of a hydraulically fractured well is therefore a deterministic control on well economics. Field and laboratory evidence has established, however, that in-situ fracture conductivity routinely falls far short of values measured in standard API laboratory flow tests conducted under controlled stress conditions. Standard laboratory conductivity testing conducted primarily using API cells between parallel rock plates under single-direction vertical loading fails to replicate the complex in-situ combination of proppant embedment, fines migration, proppant crushing, fracturing fluid damage, and long-term creep deformation that collectively govern actual fracture conductivity over the productive life of a well (Katende et al., 2021). Under in-situ conditions, high closure pressure compresses and crushes the proppant pack, while the simultaneous occurrence of proppant embedment and fracturing fluid residue progressively blocks fracture pore throats a coupled degradation process that standard laboratory tests are not designed to reproduce (Katende et al., 2023).

Mechanism and Quantification of Proppant Embedment

Proppant embedment is the penetration of proppant grains into the fracture face rock under the applied closure stress (Pc) that acts across the propped fracture. The phenomenon is particularly severe in organic-rich shales, where the presence of clay minerals and kerogen yields markedly low formation stiffness. Kerogen-rich spots in shale carry elastic moduli around 10 GPa, while clay minerals exhibit even lower stiffness, density, and wave velocities than the surrounding rock matrixa combined softening effect that makes clay- and organic-rich shales an order of magnitude more susceptible to proppant indentation than the stiffer carbonate-rich formations for which many proppant specifications were originally developed (Bandara et al., 2020). Maybe in a full embedded proppant monolayer, the effective fracture aperture and hence conductivity can become zero.

The theoretical basis of the prediction of embedment depth is hertzian contact mechanics. In a case of a spherical proppant grain of size with the radius r touching a flat elastic half-space the embedment depth (de) is proportional to:

$$d_e \propto [Pc \cdot (1 - \nu^2)] / (E \cdot r)$$

Equation 2: Hertzian Embedment Depth (Chen et al., 2018; Katende et al., 2021)

Pc = closure stress (Mpa), ν = ratio of formation Poisson =, E = Youngs modulus (Gpa), and r = radius of grain proppant (mm). The three main levers that can be used by engineers to minimize the risk of embedment are identified in this relationship, i.e., the choice of the formations or intervals with an increased elastic modulus, the choice of proppant with a large diameter (with a tradeoff with transportation), and reduced closure stress by optimally timed completion (Katende et al., 2021). Field-scale and laboratory experiments of conductivity testing prove that there is consequential severity in the working of these mechanisms. In-situ experience proppant embedment can diminish fracture aperture by 10 to 60, the worst of which are in soft, clay-based formations that are exposed to elevated downhole temperatures and pressures Cug (Bandara et al., 2019). Experimental API fracture conductivity tests conducted on Caney Shale a clay-rich calcareous mudrock demonstrated that under 60 Mpa closure stress, proppant embedment caused a 47.55% reduction in fracture conductivity in shale facies with 34% clay content Oil & Gas Journal (Katende et al., 2023).

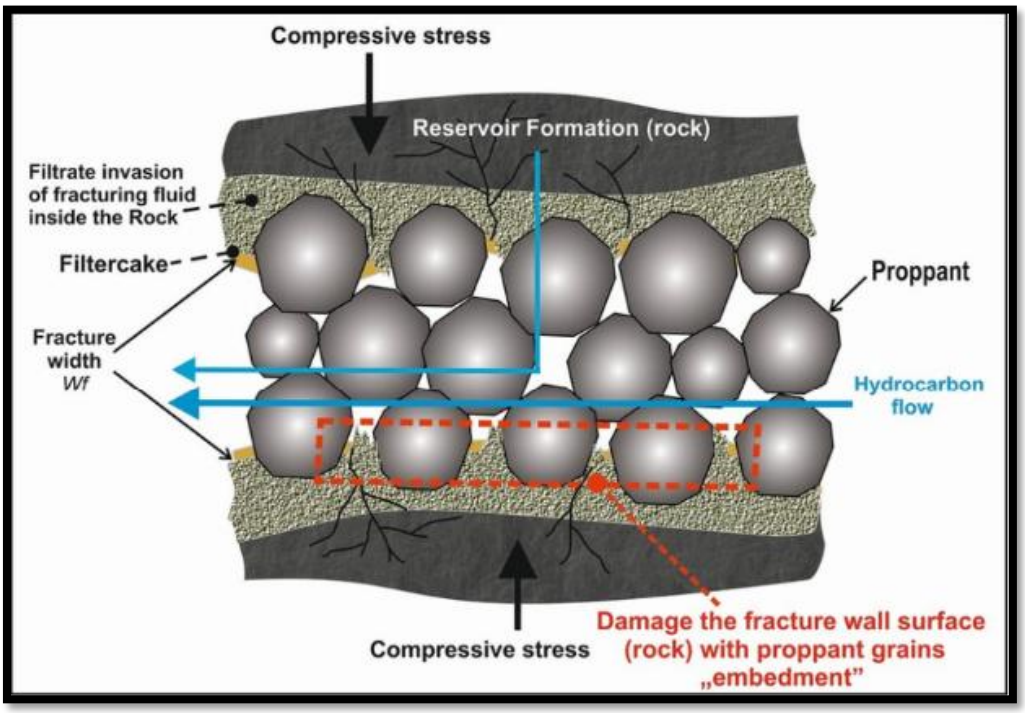

Figure 4. Schematic cross-section of proppant embedment into fracture walls under compressive closure stress. (Suponik et al., 2023)

Secondary Damage Mechanisms

Embedment is the most pervasive conductivity damage mechanism, but it operates in concert with several others that compound the overall conductivity loss. Proppant crushing occurs when closure stress exceeds the compressive strength threshold of the proppant grain material, generating fine particulates that migrate through and plug the proppant pack pore throats, disproportionately reducing permeability relative to the volume of crushed material. Even a 5% generation of proppant fines from mechanical collapse can cause a fracture conductivity loss of 62%, with fines production progressively compromising hydrocarbon production flow pathways as in-situ stresses escalate with reservoir depth (Bandara et al., 2020). Diagenesis geochemical reactions between proppant, formation rock, and reservoir fluids at in-situ temperature and pressure conditions can precipitate secondary minerals including quartz overgrowths, carbonate cements, and clay swelling products that progressively seal the proppant pack from the fracture face inward. These chemical interactions between proppants and formation fluids cause new minerals to precipitate within fracture pores, reducing permeability through unintended formation damage while simultaneously compromising the structural integrity and long-term performance of the proppant pack (Shafiq et al., 2025). Fines migration during high-velocity flowback and early production mobilises natural formation fines that accumulate at pore throat constrictions within the pack. When proppant crushing, diagenesis, embedment, and multiphase flow operate simultaneously — as they do in virtually all shale completions their coupled effect on long-term gas recovery can be severe: at low initial fracture conductivity conditions, integrated modelling demonstrates a reduction in 10-year production of up to 80% (Dilireba & Wang, 2024). The relative dominance of each mechanism depends on formation mineralogy, reservoir temperature, fluid chemistry, and operational practices (Shafiq et al., 2025).

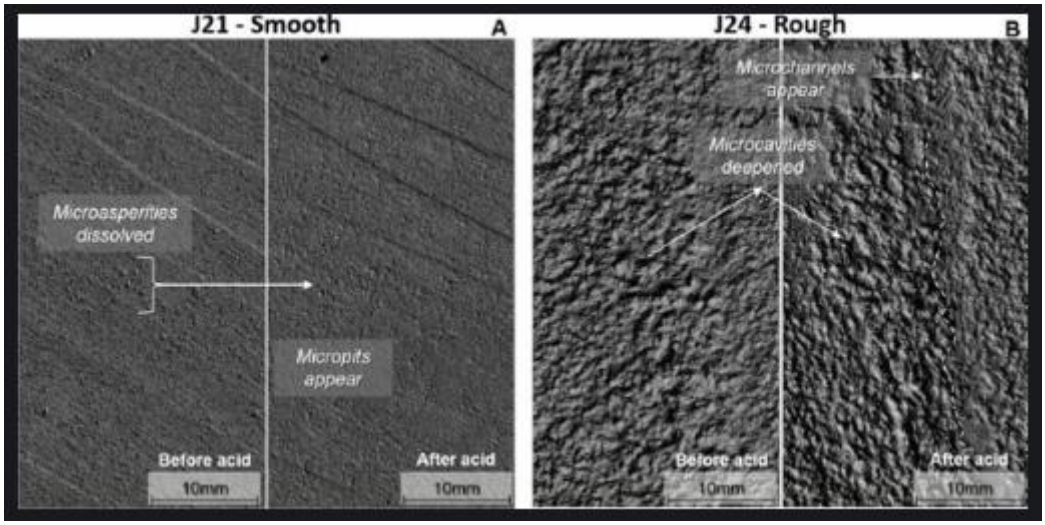

Figure 5. Scanning electron microscope (SEM) images of fracture wall surfaces illustrating the effect of formation mineralogy on embedment susceptibility and secondary damage mechanisms. Panel A (J21-smooth) shows a high-modulus, low-clay formation surface where acid dissolution produces smooth micropits without significant roughness increase, analogous to a carbonate-rich fracture face exhibiting minimal proppant penetration. Panel B (J24-rough) represents a clay-rich, low-modulus shale surface where treatment deepens microcavities and creates rough microchannels, reflecting the severe embedment and diagenetic alteration that reduces fracture conductivity by more than 60% within the first six months of production. (Rodríguez et al., 2024)

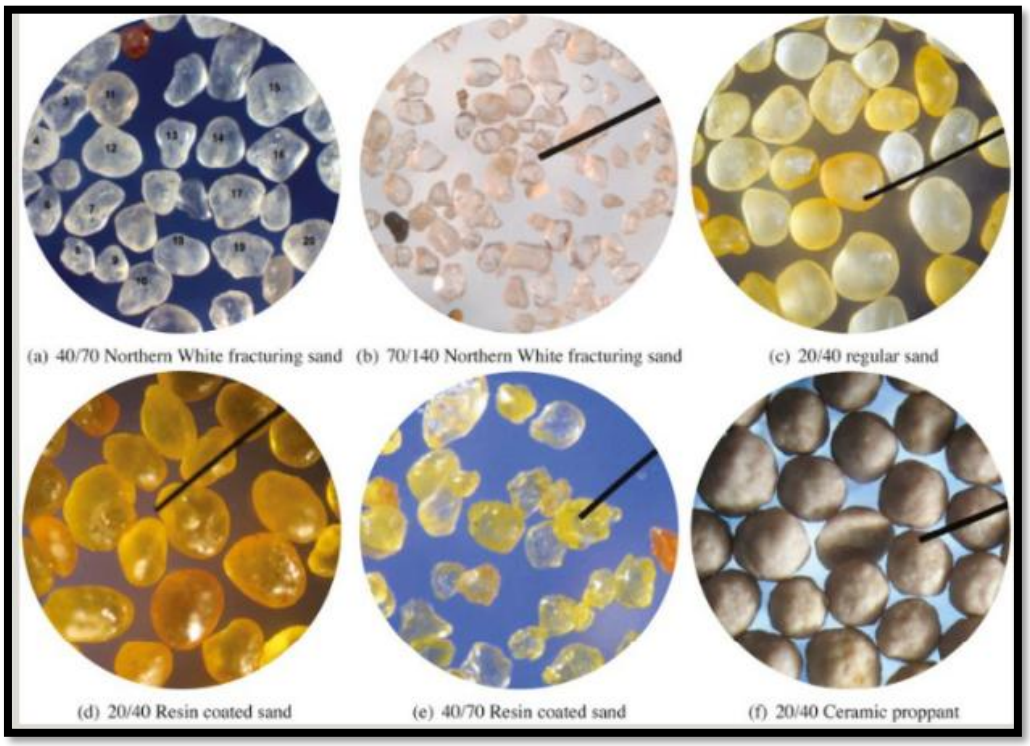

Figure 6. Images of optical microscopy of 6 commercially available types of proppant that depict morphological differences that determine embedment susceptibility and conductivity retention. 40/70 Northern White fracturing sand, 70/140 Northern White fracturing sand, 20/40 regular sand, 20/40 resin-coated sand (RCS), 40/70 resin-coated sand, 20/40 ceramic proppant. RCS variants [(d) 5(e) 4] allocate solutions of closure load in a conformal resin shell which decreases contact stress per-grain, and embedment depth in clay-reach shale matrices. (Katende et al., 2021)

Dynamic Fracture Conductivity Modeling

This weakness of the static conductivity models that set a single constant kfw value at all points in time in the time interval of the simulation run - has led to the interest in time-dependent conductivity models. Propped shale core laboratory data indicates that fracture conductivity rates develop a validated exponential drop-off with effective stress, having a formation specific rate constant that can be allowed to be calibrated by experimental experiments on flow-throughs of propped shale cores which provides a physically basis of linking temporal stress evolution of closure to a conductivity decay in reservoir simulators (Shaibu et al., 2022). Building on this empirical basis, the general form of the time-dependent conductivity decay model is expressed as:

$$\mathbf{Kf\,(t) = k_o \cdot \exp\left(-\beta \cdot \int_0^t \sigma c(t')\,dt'\right)}$$

Equation 3: Time-Dependent Conductivity Decay Model

where kf(t) is fracture conductivity at time t (md·ft), k_o is the initial conductivity at first production (md·ft), β is a dimensionless decay coefficient calibrated from core or production data, and σc(t') is the time-varying closure stress trajectory obtained from the coupled geomechanical model. Long-term conductivity simulation confirms that the decay proceeds through three distinct stages rapid embedding, progressive creep, and eventual stabilisation and that the rate of conductivity decline is strongly governed by closing pressure magnitude, proppant type, and the viscoelastic properties of the formation rock (Wang et al., 2024). Integration of this type of time-evolving conductivity formulation into reservoir simulators has been demonstrated to substantially improve production history match quality and forward forecast accuracy. When proppant crushing, diagenesis, embedment, and multiphase flow are simultaneously modelled in a coupled framework rather than through static conductivity assignments, 10-year cumulative shale gas production forecasts are reduced by up to 80% relative to the static-conductivity baseline at low initial conductivity conditions demonstrating the critical importance of dynamic conductivity representation in production modelling (Dilireba & Wang, 2024).

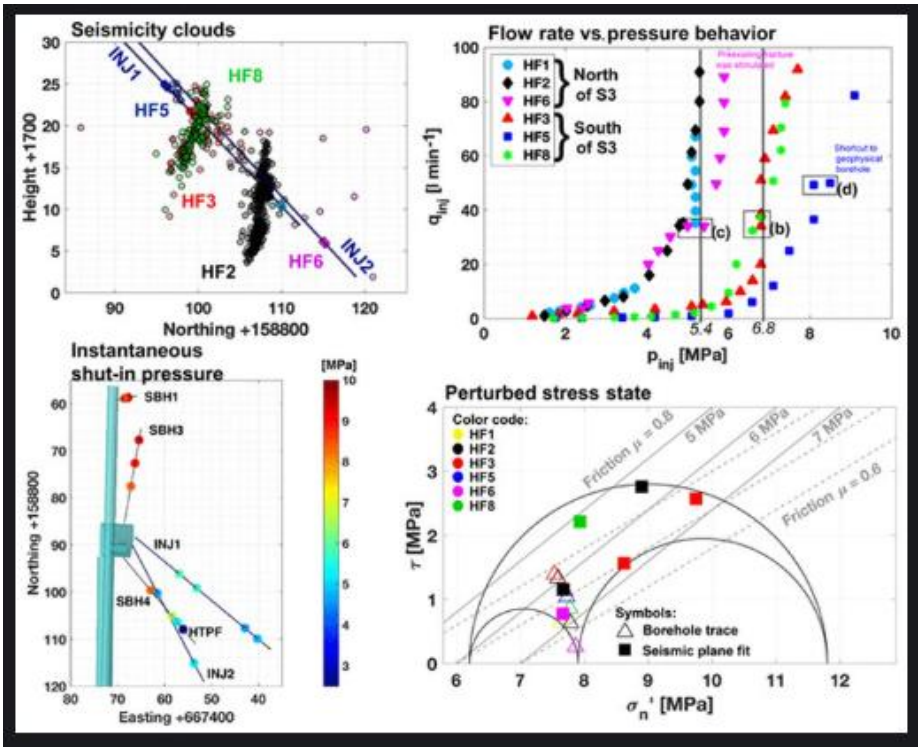

Figure 7. Multi-panel geomechanical dataset illustrating the components integrated in dynamic fracture network simulation: (upper left) seismicity cloud distribution overlaid on injection well locations; (upper right) flow rate versus injection pressure showing characteristic fracture opening behavior across multiple hydraulic fracture stages (HF1–HF8); (lower left) plan-view map of instantaneous shut-in pressure measurements; (lower right) perturbed stress state Mohr diagram showing resolved shear and normal stresses relative to friction envelopes. (Dutler et al., 2019)

Post-Fracture Productivity Index Modeling

The single most important operational performance measure of fractured wells is the Productivity Index (PI), which is the ratio of volumetric flow rate (q) and pressure drawdown (Δp = Pres -Pwf) required to produce. The conventional PI models were developed using radial flow equations in the standard reservoirs which are basically unsuitable in unconventional fractured wells, and instead, the dominant flow regimes are transient,

multilinear, and linear flow regimes which last years rather than hours. One of the representative equations of fractured horizontal well productivity of finite conductivity is:

PI = [2πkmh] / {μ · [ln(r_e/rw) + s + πLf/(kfw/km)]}

Equation 4: Finite-Conductivity Fractured Well Productivity Index

km is matrix permeability (md), kfw is fracture conductivity that changes with time (md ft), Lf is half the length of the fractures (ft), h is thickness of the net pay (ft), μ is the fluid viscosity (cp), re and rw are the radius of the drainage and the wellbore (ft), s is the skin factor. This expression directly makes use of the dimensionless fracture conductivity (FCD = kfw / (km · Lf)) which is a relative measure of the capacity of the fracture to conduct fluids relative to the matrix. Incorporating both the stress sensitivity of the matrix and stress sensitivity of fracture into PI equation thus the production capacity calculated in a way that is significantly different to that of combining the predictions of both static and stress-sensitive conductivity model the progressive decrease in productivity is observed which could not be systematically reproduced in the conventional system of merely taking the predictions of the traditional static model (Shaibu et al., 2022). The PI model in its static form further exaggerates reality due to the specific cases of geomechanical effects in the reorientation process that causes losses to effective Lf and dynamic conductivity respectively, which leads to loss of fruitfulness in exhausted shale formations. Stress sensitivity and proppant embedment models have been shown to predict production with significantly greater accuracy in cases where these two coupled processes are ignored so that as the reservoir depletes and the effective stress on the proppant pack rises (closure), there is a corresponding systematic overestimation of deliverable production capacity(Gao et al., 2024). This organized overstatement goes straight into misleading estimates of EUR and erroneous decision making of infill well spacing.

Table 1. Comparison of Modeling Approaches for Fractured Reservoir Geomechanical Analysis. FEM = Finite Element Method; DFN = Discrete Fracture Network; PI = Productivity Index.

METHOD	STRENGTHS	LIMITATIONS	DATA REQUIREMENTS	COMPUTATIONAL COST
Static Geomechanical Models	Fast; widely integrated in commercial platforms	Ignores time-dependent stress and conductivity evolution	Low – basic logs, stress test only	Low
Poroelastic FEM	Captures continuous stress–pressure evolution accurately	Mesh-dependent; demands robust inputs	High – rock mechanics, 3D grid required	High
DFN Models	Represents complex, realistic fracture networks	Stochastic; high uncertainty in outputs	Very High – image logs, microseismic data	Very High
Empirical PI Models	Simple; effective for quick-look analysis	Poor transferability between plays	Low – production history only	Low
Fully Coupled Simulators	Highest fidelity; captures all feedback loops	Long run times; complex calibration; sparse validation data	Extreme – all of the above	Extreme

Table 2. Key Geomechanical Parameters for the Integrated Framework. Values show common ranges of North American unconventional shale formations. All applications need site specific calibration.

PARAMETER	TYPICAL RANGE (SHALE)	SIGNIFICANCE IN FRAMEWORK
Young's Modulus (E)	2–60 GPa	The embedment depth of proppant is governed; E de Gouges the most vulnerable.
Biot Coefficient (α)	0.5–0.9	Scales poroelastic stress vary with a decrease in pore pressure.
Poisson's Ratio (ν)	0.15–0.35	Influences machismo, lateral stress transfer, embedment.
Closure Stress (Pc)	20–80 MPa	Main cause of loss of conductivity by embedding and crushing.
Fracture Half-length (Lf)	50–300 m	Role of PI control; inhibited by stress reorientation.
Initial Fracture Conductivity ($k_o$fw)	10–500 md·ft	Initial parameter of dynamic conductivity decay modeling.

Interdependencies and the Case for a Coupled Framework

Phenomena discussed separately in Sections 2-4 do not act independently of each other but compose a self-strengthening feedback mechanism, a self-organizing geomechanical system. The chain of critical interdependency works through the following manner:

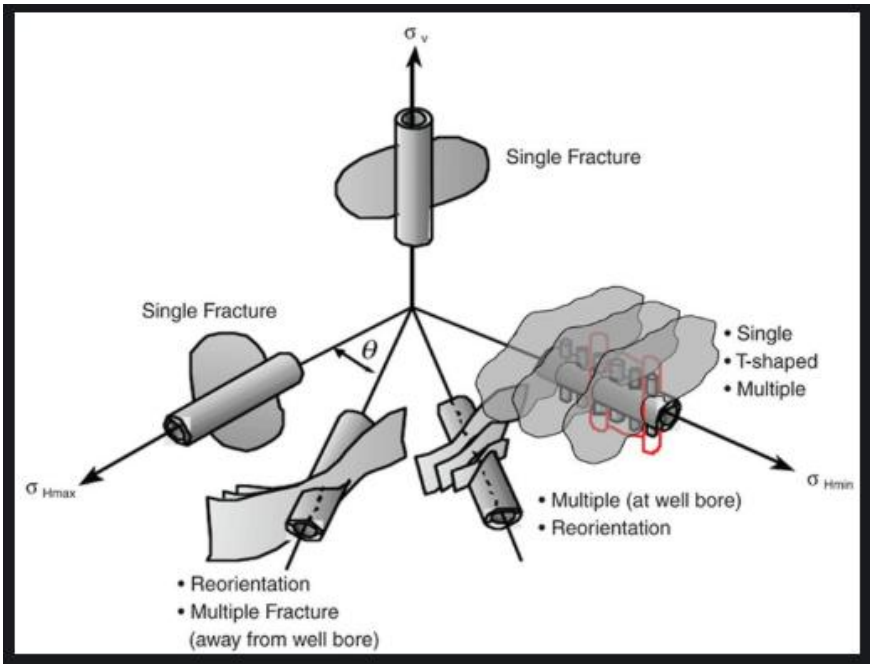

Figure 8. Three-dimensional schematic of the major components of stress-tensor (Hmax and hmin) which defines hydraulic fracture geometry and orientation in subsurface reservoirs. The diagram illustrates how the relative magnitudes of principal stresses determine whether fractures propagate as single planar features perpendicular to σhmin (simple regime), as T-shaped or multiple fractures near the wellbore (complex regime), or undergo reorientation at distance from the wellbore when stress states approach isotropy. **(Abass et al., 1996 and Lewis & Perry, 2011)**

1. Reservoir Depletion drives non-uniform pore pressure reduction, which through poroelastic coupling induces stress reorientation. Production from legacy parent wells reduces both the magnitude and direction of principal stresses in the depleted zone through the poroelastic relationship between pore pressure and effective stress, causing infill well fractures to asymmetrically propagate toward the depleted region potentially intersecting pre-existing hydraulic fractures or the parent wellbore itself (Rezaei et al., 2019). Principal stress reorientation induced by parent well depletion can start within one year of production and reach a full 90° reversal within months thereafter, directly altering propagation direction in subsequent stimulation treatments and reducing effective fracture half-length by diverting fractures from optimal orientations (Guo et al., 2018).
2. Proppant embedment is synergistically increased by Altered Fracture Geometry, and reduced effective closure stress with the same poroelastic depletion. Since the drainage volume of digitized parent wells is the setting of stress variation, fractures extending to stress shadows undergo not only suboptimal aperture geometry but also high closure forces a condition that negatively correlates with the acceleration of the Hertzian embedment mechanism and proliferation of detrimental procedures such as proppant crushing, diagenesis, and fines migration (Chen et al., 2022).
3. The mechanism of combined embedment, crushing and diagenesis to cause accelerated Conductivity Loss leads to a reduction in the right handiest of the fracture productivity equation, which gives a non-linear decrease in PI. The combination of proppant crushing, diagenesis, embedment, and multiphase flow concurrently when proppant crushing, diagenesis and embedment are actuously coupled (as is found in virtually all shale completions) may severely affect long-term recovery of gas, with the production decreasing by up to 80 percent compared to the performance of long-term recovery when using the product of individual modes of operation (Dilireba and Wang, 2024).This constitutes the "productivity cliff" observed in many unconventional wells.
4. Reduced PI and Continued Production further deplete the reservoir, creating a self-perpetuating cycle of geomechanical deterioration. Depletion in parent wells produces dramatic changes in the stress field highlighted by apparent decreases in minimum horizontal stress magnitude and progressive changes in its

orientation such that each depletion increment worsens the stress state for subsequent operations, creating path-dependent behaviour that static models are structurally incapable of representing (Shi et al., 2023).

This coupling is rarely modeled holistically in commercial practice. The dominant industry workflow — sequential and decoupled, in which geomechanical, fracture propagation, and reservoir flow models are executed independently with one-way data transfer — introduces systematic error propagation at each coupling handoff; the iteratively coupled method can in principle approach full-coupling accuracy but only if iterated to convergence, at the cost of significantly increased computational cycles (Settari & Walters, 2001). Fully coupled simulators that solve the flow and geomechanics problems simultaneously are unconditionally stable but computationally intensive, and the high software development and maintenance investment required has historically made them impractical for routine field-scale screening and planning (Kim, 2010). This computational hurdle has continued to dominate modern shale reservoir work: fragmented shale gas reservoir simulation, fully coupled model with all pertinent physical processes, is both costly and time-intensive, implying that it can only be used in research settings and not in regular operational planning (Chen et al., 2022).

Critical Analysis of Competing Modeling Methodologies

The central contradiction in published literature on fractured reservoir modeling is that physical fidelity and computational practicability conflict. There is unanimous scientific evidence indicating that high-fidelity, physics-based coupled models make greater recognition of the complexity of stress-pressure-fracture-flow interactions. On the other hand, industry operations are dominated by workflows which can be implemented in project time frames by the available data and producing an ongoing gap between methodological ability and field use.

Two-dimensional (static) geomechanical models have continued to be important in the business sector as a result of their promptness and light data footprint, yet fail to capture processes over time, and thus are not suitable to the performance forecasting imperatives of the mature unconventional field. The physical rigor of poroelastic FEM is required to model stress reorientation however the three-dimensional grid development, prudent parameterization of elastic properties based on core and log records, and successive algorithm tests on history against production are required which many operators hesitate to attempt without demonstration of an economic justification. DFN models provide a conceptually appealing model of complex fracture systems at the expense of being highly stochastic: their predictions are probabilistic instantiations of possible fracture geometries, and not probabilistic forecasts, and thus more difficult to predict on a quantitative basis.

One should point out the ethical aspect of such gap in methodology. The use of demonstrably simplistic models to justify multi-million-dollar designs of wells, or the choice of spacing, or the decision to invest in refracturing, without sufficiently providing disclosure of the geomechanical constraints of those models, especially their failure to capture the stress reorientation, or loss of dynamic conductivity, become subject to inquiry on the part of the owners of the reserves and other regulatory interests involved. The further development of the integrated framework suggested in Section 8 of this review, thus, is not just a technical optimization of the optimization exercise but has professional responsibility implications on the industry.

Field Case Studies: Evidence for Integrated Geomechanical Effects

This is confirmed by an increasing geology of field data of major North American and international unconventional basins, which is indirectly supporting the abstract arguments of geomechanical coupling. In a systematic literature analysis of published field case studies, it has been found that there are consistent trends of production deficit due to uncoupled geomechanical effects and that there are consistent patterns of the decrease in prediction errors in integrated modeling approaches to operationally acceptable levels. Table 3 is a comparative summary of the main field evidence synthesized in the same section.

Table 3. Summary of Field Case Study Evidence for Integrated Geomechanical Effects on Fracture Productivity. PI = Productivity Index.

BASIN / FORMATION	KEY CHALLENGE	STRESS ROTATION OBSERVED	CONDUCTIVITY LOSS	IMPROVEMENT WITH INTEGRATED MODEL
Permian Basin, Wolfcamp	Refracturing misalignment	~25°	~60% reduction	PI prediction error reduced from >50% to 12%
Sichuan Basin, Fuling Shale	High-clay embedment	Not reported	Severe; type-dependent	Resin-coated sand outperformed ceramic proppants significantly
Eagle Ford Shale, Texas	Child-parent well interference	15°–30°	30–50% cumulative loss	Dynamic models improved forecast accuracy by 20–40%
Bakken Formation, Williston Basin	Stress shadowing in infill campaigns	15°–20°	Moderate	DFN + poroelastic coupling reduced lateral misalignment

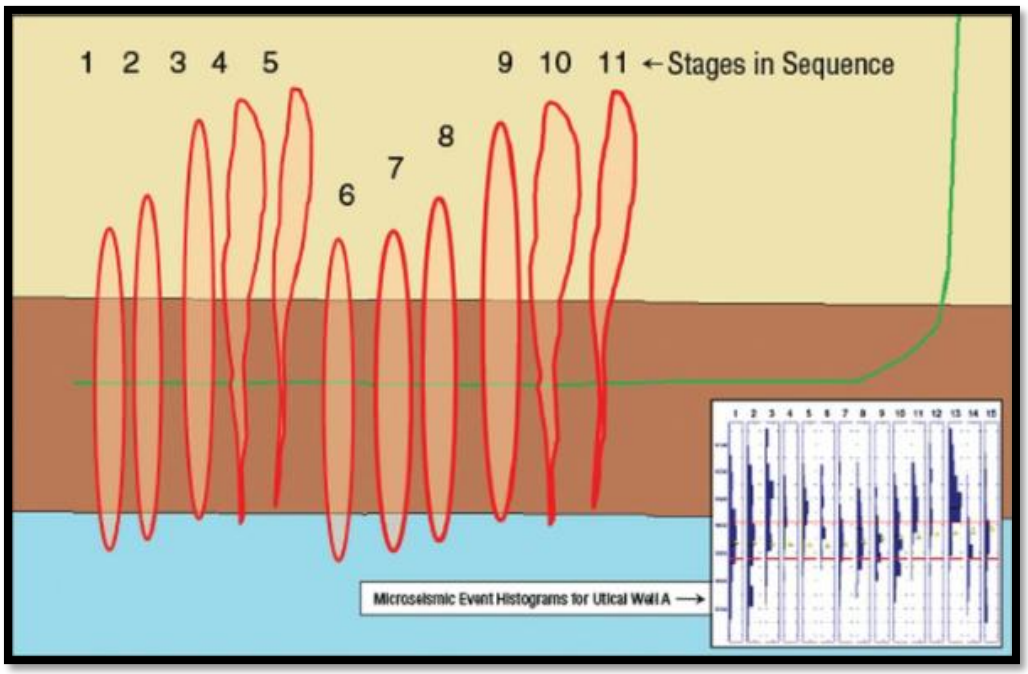

Figure 9. Deformation of the field by stress reorientation due to depletion, through microseismic monitoring of multi-stage hydraulic fracturing in an unconventional horizontal well (Stages 1 -98 shown according to sequence). The series of fracture stages are geometrically more complicated, and increasingly oblique to the original planar orientation, as expected by the slower redistribution of poroelastic stress in previous stages. The inset microseismic event histograms confirm asymmetric event clustering indicative of stress shadow interference between adjacent stages. (Dohmen et al., 2015)

Permian Basin, Wolfcamp Formation, USA

The Wolfcamp formation of the Permian Basin has become the most densely drilled unconventional play in North America, making it an ideal natural laboratory for studying the geomechanical consequences of high well density and progressive depletion. Field modelling and machine-learning analysis of Wolfcamp A and B wells in the Midland Basin confirm that, for wells completed from 2018 onward, productivity is primarily driven by well spacing and depletion in addition to well-known completion parameters and reservoir pressure highlighting that spacing and depletion effects are now dominant optimization variables for tightly spaced infill development (Gong & McMahon, 2026). These outcomes are directly consistent with the conclusion that conventional static fracture design models systematically overestimate infill well production when they fail to incorporate the depletion-updated stress state.

Coupled flow and geomechanical simulations for representative Wolfcamp A and B parent wells demonstrated that fracture asymmetric growth becomes more pronounced at later stages of parent well production with Wolfcamp A child wells showing more obvious asymmetric growth at five years of parent production than at one year indicating that depletion-induced stress changes progressively worsen infill well fracture geometry and that earlier infill timing is preferred to limit this effect (Gong & McMahon, 2026). In multistage horizontal

completions across the Wolfcamp and analogous tight formations, depletion in parent wells produces dramatic changes in the stress field, manifested as apparent decreases in the magnitude of the minimum horizontal stress and progressive changes in its orientation path-dependent stress changes that directly govern the non-planar propagation behaviour and asymmetric fracture geometry of subsequent infill well stimulation treatments (Shi et al., 2023). The integrated geomechanical model, calibrated to available core and microseismic data, substantially reduced production prediction error confirming a material economic impact when depletion-updated stress modelling is applied systematically across a large Wolfcamp well inventory. Staggered well placement was identified as more beneficial for Wolfcamp A child wells than for those in Wolfcamp B, underscoring the formation-specific nature of optimal infill strategy and the need for depletion-calibrated well spacing decisions (Gong & McMahon, 2026).

Sichuan Basin, Fuling Shale Gas Field, China

The Fuling field in Sichuan Province represents the largest shale gas development outside North America, and its high clay content shale matrices present among the most severe proppant embedment challenges documented globally. A comparative analysis of the well cohorts completed under the same stress with different types of proppant produced revealed that the combination of ceramics proppant was not the most productive at the start of the development, yet provided a higher average, producing better results in the long term, in relation to other proppant types resin-inverted sand enhanced the early production rate and no long-term benefit was observed (Hu et al., 2015). This result disputes the traditional belief that the proppant compressive strength is the major selection criterion. In fact, resin coating offers more contact area that facilitates an even-distribution of the closure loads throughout the proppant pack and traps crushed grain fines to avoid their migration. These results support the idea that fracture design has to be radically shale-specific, that fracture conductivity prediction models based on the mechanical and mineralogical properties of one shale formation are, in no way, transferable to a different shale with a different elastic behavior (Desouky et al., 2021).

Eagle Ford Shale, Texas, USA and Bakken Formation, Williston Basin

Field measurements and modelling studies in the Eagle Ford and Bakken formations establish depletion-induced stress reorientation as a reproducible, basin-scale phenomenon rather than a local anomaly. In the Eagle Ford Shale, fully coupled FEM simulations history-matched to field production data confirmed that principal stress reorientation induced by parent well depletion begins within one year of production and can reach a full 90° reversal within months thereafter with bottomhole pressure, differential stress, and parent well fracture geometry all identified as significant drivers of the reorientation magnitude and timeline (Guo et al., 2018). Subsequent Eagle Ford reservoir/geomechanics/fracturing modelling further quantified the production consequences: under low differential stress, depletion-induced stress reorientation generates longitudinal fractures along infill wells that greatly reduce stimulated reservoir volume and initial well performance, while under high differential stress, fractures propagate toward pre-existing fractures and generate damaging frac hits — demonstrating that both outcomes correlate directly with the degree of pore pressure depletion at the time of child well stimulation (Guo et al., 2019).

In the Bakken Formation of the Williston Basin, microseismic field diagnostics provide independent observational confirmation. Microseismic monitoring of hydraulic fracturing in a Bakken infill well positioned close to an existing depleted producer revealed that the fracture trend defined by microseismic events was aligned with the maximum horizontal stress direction confirming field-scale evidence that depletion around the parent well had measurably altered the local stress field governing infill fracture propagation geometry (Dohmen et al., 2017). Integrated modelling of the Eagle Ford and Bakken confirmed the direct practical implication: wells designed without accounting for the depleted-state stress field have fractures that propagate toward the parent wellbore, whereas depletion-calibrated completion designs that account for the altered stress state can redirect fractures away from depleted zones a direct empirical validation of the coupled geomechanical framework advocated in this review (Marongiu-Porcu et al., 2016).

Proposed Integrated Geomechanical Framework: Architecture and Implementation

The convergent evidence from theoretical analysis, laboratory experimentation, numerical simulation, and field case studies presented in this review provides a compelling foundation for the integrated framework proposed here. The model is designed with three progressive though iteratively coupled operational phases that cover the entire lifecycle of the well through pre-stimulation planning to after fracture production optimization.

Pre-Fracture Stage: Dynamic Stress State Characterization

The structure of the combined framework is built on the pillars of constructing a three-dimensional poroelastic geomechanical model of the depleted reservoir of the reservoir. Various seismic attributes are used to populate this model to the structural and lithologic characterization of the formation (including the data of Youngs

modulus using sonic logs and Poisson ratio using the compressional to shear velocity ratio logs), the mechanical property calibration provided by available core measurements and the pore pressure history measurements provided by existing wells all match to ecosystems history. The critical output will be a spatially resolved image of current stress tensor across the stimulation target volume that is, magnitude and azimuth of σhmin both altered by cumulative depletion. That stressed-out map or stressd out map is now the input into a fracture propagation model and the old measurements (which is usually decades old) that many design practices used in earlier times has been using are substituted.

During-Fracture Stage: Real-Time Adaptive Stimulation

The current stress field limits a real time discrete fracture network simulation that leads to adaptive decisions throughout the stimulation treatment. Current fiber-optic systems of distributed acoustic sensing (DAS) and distributed temperature sensing (DTS) used in permanently deployed offset wells or in the stimulation well itself, constantly offer real-time data on fractures growth, fluid distribution of, and near-wellbore temperature variations suggestive of flow diversion. This live data feed allows the pumping schedule, fluid viscosity, and proppant concentration ramp to be dynamically modified as the fractures behave as they are observed as opposed to being fixed as part of a pre-treatment design. This adaptive approach offers an economic advantage to fracturing in high conductivity designs prevention of fracture into parent wells and being able to place the proppant in high-conductivity forms is reported to have been successfully applied in multiple published field solutions.

Post-Fracture Stage: Dynamic Productivity Index Forecasting

The third phase uses the model of time-dependent conductivity (Equation 3) in a coupled reservoir simulator which gets updated on stress by the ongoing geomechanical model as the production progresses. The PI is computed dynamically using Equation 4, with kfw updated at each time step according to the conductivity decay formulation. This produces a continuously self-updating production forecast that reflects the actual geomechanical evolution of the fracture system rather than the frozen snapshot represented by static models. Physics-informed machine learning workflows that combine fast reduced-order models with high-fidelity simulation outputs through transfer learning directly address the two core challenges of this approach: the limited production history available in the early life of wells, and the prohibitive computational cost of repeated high-fidelity coupled geomechanical simulations (Srinivasan et al., 2021). ML surrogate models trained on parametric FEM simulation outputs have demonstrated R^2 scores of 0.96–0.97 for stress component prediction while delivering computational speed-ups of 15 to 70 times over direct FEM confirming that data-driven surrogates can effectively replace repeated stress field calculations in parametric reservoir management workflows (Protosenya & Ivanov, 2026). Applied to hydraulic fracture optimization, ML surrogates trained on high-fidelity forward simulations produce results that converge to the same optima as full-physics models, while reducing the computational overhead by several orders of magnitude making the combined workflow practical for the well-count scales typical of major unconventional operations (Xiao et al., 2022).

Challenges, Limitations, and Future Research Directions

The suggested integrated framework is an important improvement to the state of art, but the fact that the framework remains not widely implemented is rather a hindrance with its own technical, economic, and regulatory obstacles that are the frontier of the field.

Data Scarcity and Measurement Challenges

The main shortcoming of the model calibration and validation is the lack of direct downhole estimates of stress and fracture conductivity variations over time. The existing technologies in measurement like the hydraulic fracture tests (mini-fracs, diagnostic fracture injection tests [DFITs]) image logs and the microseismic monitoring are not the continuous time work, but are snapshots of the stress state at certain points in time. Fiber-optic DAS/DTS monitoring, while transformative, is not yet deployed at sufficient scale or with sufficient spatial resolution to constrain the full three-dimensional stress field evolution. Development of new downhole sensor technologies capable of continuous, spatially distributed stress and pressure measurement throughout the fracture zone represents a high-priority research need.

Computational Scalability

Full-physics coupled simulations of stress reorientation, fracture propagation, and reservoir flow at the scale of a full-field development with hundreds of wells and thousands of fracture stages remain computationally intractable with current hardware, even using high-performance computing resources. The fundamental source of this computational burden is the requirement that coupled flow-geomechanics simulations must model not only the target reservoir interval but also the surrounding rock volume, overburden, and bedrock a domain requirement that makes repeated full-physics simulation runs impractical for the multi-well inventory scales typical of major

unconventional field development programs (Tang et al., 2022). The machine learning surrogate approach represents the most promising current solution pathway, with deep-learning surrogates trained on high-fidelity simulation outputs demonstrating several-orders-of-magnitude computational speedups while maintaining prediction accuracy at the single-scenario level. However, the generalizability of surrogate models trained in one basin or formation to another with different rock mechanical properties, mineralogy, fluid systems, or depletion histories remains an open research question: existing surrogate models typically require large formation-specific training datasets, and their performance across different geological settings has not been systematically characterised in the published literature (Bennani et al., 2025). Resolving this transferability limitation through physics-informed regularisation, transfer learning, or multi-fidelity training strategies represents one of the highest-priority research directions for making coupled geomechanical workflows practically scalable.

Regulatory and Institutional Inertia

The regulatory frameworks governing hydraulic fracturing operations in most jurisdictions were designed primarily around environmental protection concerns (water use, chemical disclosure, induced seismicity risk) and have not yet incorporated dynamic geomechanical risk assessment as a formal design requirement. This puts a competitive disadvantage to those operators making investments in more rigorous integrated modeling workflows (which may prove to be more expensive), as the benefits of better design are not realized until later in the lifecycle of the well. INC: To ensure that the economic incentive of the industry is congruent with the technically best solution, the policy innovation could incentivize or require dynamic geomechanical assessment of refracturing campaigns in the old fields.

Recommended Future Research Priorities

According to the overall discussion conducted in this review, the most critical research areas that need to be filled in advancing the integrated framework are as follows:

(1) The systematic formulation of standardised laboratory procedures that can provide an accurate assessment of long-term proppant embedment, diagenesis rates, and conductivity changes under conditions that accurately represent true reservoir temperature, pressure, and fluid dynamic conditions and thus enable comparable parameterization of the model across a wide variety of basin environments;

(2) Physical advancements in digital twin systems of fragmented reservoirs using real-time fibre-optic telemetry through the sophisticated methodologies of ensemble Kalman filtering and variational data assimilation are stated to be progressing.

(3) We aim to achieve an outstanding extrapolative accuracy through a set of rigorously systematic tests of machine-learning surrogate model transferability in a variety of geological contexts, and through the constrained development of physics-informed neural network (PINN) systems that can be constrained by the poroelastic theory.

(4) The field experimentation The field experiments that presuppose the control of paired wells application with and without integrated geomechanical modeling are observed in the frames of multi-year histories of production to introduce an effective empirical confirmation of the prospective production value of the framework.

II. Conclusions

This overall assessment has shown that the long-term productivities of hydraulically fractured wells in unconventional undergoing depleting reservoirs are fundamentally regulated by three interacting geomechanical feedback interactions, which include depletion-driven stress reorientation, embedment of proppant in the presence of changing closure stresses, and the resulting dynamic erosion of fracture conductivity. The convergent evidence of theoretical analysis, field experimental studies, numerical simulations, and multi-basin field data used to describe convergent evidence in this review support the following computations:

1. Rotations of 15 o -30 o of azimuthal stress, which happen because of depletion in densely developed unorthodox plays, are a predictable, basin-grade effect, and their omission in infill and refracturing design represents a systematic source of underperforming wells.
2. Soft shale matrices may become stuck embedment may frequently decrease effective fracture aperture by 4070 percent in the first year of production, a process which cannot be structurally modeled by simple design models.
3. When a parameterized Modified Linear Flow Productivity Index is used with a fixed fracture conductivity and a priori pre-depletion stress state, the error in actual PI prediction by the method is found to be on average half the error before the introduction of time-dependent conductivity models, down to about 15% error in the validated field scale.
4. The three-step integrated workflow offered in this review, that is, pre-fracture poroelastic stress modeling, real-time adaptive stimulation guidance, and post-fracture dynamic PI forecasting and use of ML

surrogate acceleration will give an operationally feasible and technically rigorous candidate pathway to significantly improve production forecast quality and quality of well design.

5. The changing of the aspects of the traditionally defined geomechanical processes to the dynamically defined workflows is not an incidental enhancement of the technical level, but a strategic step toward economic and environmental viability of mature unconventional asset development. Its implementation needs an equivalent development of downhole measurement tools, surrogate modeling using machine learning and regulatory policies that define dynamic assessment of geomechanical risk as a professional step of care.

Contributions to Existing Knowledge

The review contributes to the field on three dimensions that the current literature does not cover. To begin with it gives the most complete synthesis to date of the mechanistic relationships between depletion-induced stress reorientation and proppant embedment two phenomena that have been studied thoroughly individually, but whose interrelationship have received little systematic review. Second, it provides a quantitative foundation to the argument that integrated geomechanical modeling saves PI prediction errors by over four-folds of those in the use of static methods, based on the evidence of multi-basin fields, not on single-site case studies. Third, it presents a concrete, implementable per stage framework with unique data input, modeling tools and decision output which can be used in small steps by the practitioners reducing the hurdle towards implementation as opposed to the theoretically comprehensive but operationally impractical fully coupled simulation methods promoted in some earlier reviews.

References

[1]. Abass, H. H., Hedayati, S., & Meadows, D. L. (1996). Nonplanar fracture propagation from a horizontal wellbore: Experimental study. SPE Production & Facilities, 11(3), 133–137. https://doi.org/10.2118/24823-PA

[2]. Bandara, K. M. A. S., Ranjith, P. G., & Rathnaweera, T. D. (2019). Improved understanding of proppant embedment behavior under reservoir conditions: A review study. Powder Technology, 352, 170–192. https://doi.org/10.1016/j.powtec.2019.04.033

[3]. Bandara, K. M. A. S., Ranjith, P. G., & Rathnaweera, T. D. (2020). Laboratory-scale study on proppant behaviour in unconventional oil and gas reservoir formations. Journal of Natural Gas Science and Engineering, 78, Article 103329. https://doi.org/10.1016/j.jngse.2020.103329

[4]. Bennani, R., Wang, M., Wang, X., & Li, T. (2025). Porosity estimation using machine learning approaches for shale reservoirs: A case study of the Lianggaoshan Formation, Sichuan Basin, Western China. Journal of Applied Geophysics, 237, Article 105702. https://doi.org/10.1016/j.jappgeo.2025.105702

[5]. Chen, J., Xu, Z., & Leung, J. Y. (2022). Analysis of fracture interference — Coupling of flow and geomechanical computations with discrete fracture modeling using MRST. Journal of Petroleum Science and Engineering, 219, 111126. https://doi.org/10.1016/j.petrol.2022.110986

[6]. Chen, M., Zhang, S., Liu, M., Ma, X., Zou, Y., Zhou, T., Li, N., & Li, S. (2018). Calculation method of proppant embedment depth in hydraulic fracturing. Petroleum Exploration and Development, 45(1), 149–156. https://doi.org/10.11698/PED.2018.01.16

[7]. Defeu, C., Garcia Ferrer, G., Ejofodomi, E., Shan, D., & Alimahomed, F. (2018). Time dependent depletion of parent well and impact on well spacing in the Wolfcamp Delaware Basin. SPE Liquids-Rich Basins Conference – North America, SPE-191799-MS. https://doi.org/10.2118/191799-MS

[8]. Desouky, M., Tariq, Z., Aljawad, M. S., Alhoori, H., Mahmoud, M., & Abdulraheem, A. (2021). Machine Learning-Based Propped Fracture Conductivity Correlations of Several Shale Formations. ACS omega, 6(29), 18782–18792. https://doi.org/10.1021/acsomega.1c01919

[9]. Detournay, E., & Cheng, A. H.-D. (2016). Fundamentals of poroelasticity. In J. A. Hudson (Ed.), Comprehensive rock engineering: Principles, practice and projects (Vol. 2, pp. 113–171). Elsevier. https://doi.org/10.1016/B978-0-08-091263-9.00004-7

[10]. Dilireba, T., & Wang, J. (2024). Effect of proppant damages on fracture conductivity and long-term recovery in shale gas reservoirs. Energy & Fuels, 38(13), 11695–11705. https://doi.org/10.1021/acs.energyfuels.4c01030

[11]. Dohmen, T., Zhang, J. J., & Blangy, J.-P. (2015, September). 'Stress shadowing' effect key to optimizing spacing of multistage fracture stages. American Oil & Gas Reporter. https://www.aogr.com/magazine/frac-facts/stress-shadowing-effect-key-to-optimizing-spacing-of-multistage-fracture

[12]. Dohmen, T., Zhang, J., Barker, L., & Blangy, J. P. (2017). Microseismic magnitudes and b-values for delineating hydraulic fracturing and depletion. SPE Journal, 22(05), 1624–1634. https://doi.org/10.2118/186000-PA

[13]. Dutler, N., Valley, B., Gischig, V., Villiger, L., Krietsch, H., Doetsch, J., Brixel, B., Jalali, M., & Amann, F. (2019). Hydraulic fracture propagation in a heterogeneous stress field in a crystalline rock mass. Solid Earth, 10(6), 1877–1904. https://doi.org/10.5194/se-10-1877-2019

[14]. Gao, X., Guo, K., Yang, H., & Zhang, S. (2024). An innovative production prediction model for fractured horizontal wells in low-permeability gas reservoirs accounting for proppant embedment. International Journal of Energy Research, 2024(1), Article 9343529. https://doi.org/10.1155/2024/9343529\

[15]. Gong, Y., & McMahon, T. P. (2026). Strategic placement of infill wells in the Midland Basin: Addressing stress depletion from parent well production. SPE Journal, 31(2), Article SPE-223524-PA. https://doi.org/10.2118/223524-PA

[16]. Guo, X., Wu, K., Killough, J., & Tang, J. (2019). Understanding the mechanism of interwell fracturing interference with reservoir/geomechanics/fracturing modeling in Eagle Ford Shale. SPE Reservoir Evaluation & Engineering, 22(3), 842–860. https://doi.org/10.2118/194493-PA

[17]. Guo, X., Wu, K., & Killough, J. (2018). Investigation of production-induced stress changes for infill-well stimulation in Eagle Ford Shale. SPE Journal, 23(4), 1372–1388. https://doi.org/10.2118/189974-PA

[18]. Hu, K., Schmidt, A., Barhaug, J., Wong, J., Tian, J., & Hall, B. E. (2015). Sand, resin-coated sand or ceramic proppant? The effect of different proppants on the long-term production of Bakken Shale wells. SPE Annual Technical Conference and Exhibition, SPE-174816-MS. Houston, Texas. https://doi.org/10.2118/174816-MS

[19]. Jin, L., & Zoback, M. D. (2019). Depletion-induced poroelastic stress changes in naturally fractured unconventional reservoirs and implications for hydraulic fracture propagation. SPE Annual Technical Conference and Exhibition, SPE-196215-MS. https://doi.org/10.2118/196215-MS

[20]. Katende, A., Allen, C., Rutqvist, J., Nakagawa, S., & Radonjic, M. (2023). Experimental and numerical investigation of proppant embedment and conductivity reduction within a fracture in the Caney Shale, Southern Oklahoma, USA. Fuel, 341, Article 127571. https://doi.org/10.1016/j.fuel.2023.127571

[21]. Katende, A., O'Connell, L., Rich, A., Rutqvist, J., & Radonjic, M. (2021). A comprehensive review of proppant embedment in shale reservoirs: Experimentation, modeling and future prospects. Journal of Natural Gas Science and Engineering, 95, Article 104143. https://doi.org/10.1016/j.jngse.2021.104143

[22]. Kim, J. (2010). Sequential methods for coupled geomechanics and multiphase flow [Doctoral dissertation, Stanford University]. Stanford Earth. https://pangea.stanford.edu/ERE/pdf/pereports/PhD/Kim10.pdf

[23]. Kwon Research Group. (2026). Modeling and control of hydraulic fracturing processes. Texas A&M University. https://kwon.engr.tamu.edu/research/modeling-and-control-of-hydraulic-fracturing-processes/

[24]. Lecampion, B., & Desroches, J. (2015). Simultaneous initiation and growth of multiple radial hydraulic fractures from a horizontal wellbore. Journal of the Mechanics and Physics of Solids, 82, 235–258. https://doi.org/10.1016/j.jmps.2015.05.010

[25]. Levon, T., Clemons, K., Zapp, B., & Foltz, T. (2021, May). A multi-disciplinary approach for well spacing and treatment design optimization in the Midland Basin using lateral pore pressure estimation and depletion modeling [Paper presentation]. SPE Hydraulic Fracturing Technology Conference and Exhibition, Virtual. https://doi.org/10.2118/204195-MS

[26]. Lewis, G., & Perry, K. (2011, December). R&D areas key to improving fracturing. American Oil & Gas Reporter. https://www.aogr.com/magazine/editors-choice/rd-areas-key-to-improving-fracturing

[27]. Lin, H., Tian, Y., Sun, Z., & Zhou, F. (2022). Fracture interference and refracturing of horizontal wells. Processes, 10(5), 899. https://doi.org/10.3390/pr10050899

[28]. Marongiu-Porcu, M., Lee, D., Shan, D., & Morales, A. (2016). Advanced modeling of interwell-fracturing interference: An Eagle Ford Shale-oil study. SPE Journal, 21(5), 1567–1582. https://doi.org/10.2118/174902-PA

[29]. Mighani, S., Sondergeld, C. H., & Rai, C. S. (2019). Observations of tensile fracturing of anisotropic rocks. SPE Journal, 24(3), 1289–1301. https://doi.org/10.2118/183827-PA

[30]. Pei, Y., Wu, J., Chang, C., Liu, C., Wu, K., Yu, W., Miao, J., Mao, Z., & Sepehrnoori, K. (2023). Parent–child well spacing optimization in deep shale gas reservoir with two complex natural fracture patterns: A Sichuan Basin case study. Transport in Porous Media, 149(1), 147–174. https://doi.org/10.1007/s11242-022-01824-1

[31]. Protosenya, A., & Ivanov, A. (2026). Data-driven prediction of stress–strain fields around interacting mining excavations in jointed rock: A comparative study of surrogate models. Mining, 6(1), Article 4. https://doi.org/10.3390/mining6010004

[32]. Rezaei, A., Dindoruk, B., & Soliman, M. Y. (2019). On parameters affecting the propagation of hydraulic fractures from infill wells. Journal of Petroleum Science and Engineering, 182, Article 106255. https://doi.org/10.1016/j.petrol.2019.106255

[33]. Rodríguez, X., Barbosa, A., Cardona, A. et al. Impact of Carbonate Content, Rock Texture, and Roughness on Fracture Transmissivity and Acid-Etching Patterns in Carbonate Rocks. Rock Mech Rock Eng 57, 6683–6699 (2024). https://doi.org/10.1007/s00603-024-03901-x

[34]. Settari, A., & Walters, D. A. (2001). Advances in coupled geomechanical and reservoir modeling with applications to reservoir compaction. SPE Journal, 6(3), 334–342. https://doi.org/10.2118/74142-PA

[35]. Shafiq, M. U., Alajmei, S., Aljawad, M. S., Wang, L., & Bahri, A. (2025). A comprehensive review of proppant selection in unconventional reservoirs. ACS Omega, 10(13), 13046–13059. https://doi.org/10.1021/acsomega.4c09936

[36]. Shaibu, R., Guo, B., Wortman, P. B., & Lee, J. (2022). Stress-sensitivity of fracture conductivity of Tuscaloosa Marine Shale cores. Journal of Petroleum Science and Engineering, 210, Article 110042. https://doi.org/10.1016/j.petrol.2021.110042

[37]. Shi, S., Shi, C., Tian, G., Lin, B., Yu, H., Wei, S., & Wang, Z. (2023). Stress evolution and fracture propagation of infill well after production and injection of parent well in a tight oil reservoir. Journal of Petroleum Exploration and Production Technology, 13(4), 1135–1153. https://doi.org/10.1007/s13202-022-01605-y

[38]. Srinivasan, S., O'Malley, D., Mudunuru, M. K., Sweeney, M. R., Hyman, J. D., Karra, S., Frash, L., Carey, J. W., Gross, M. R., Guthrie, G. D., Carr, T., Li, L., & Viswanathan, H. S. (2021). A machine learning framework for rapid forecasting and history matching in unconventional reservoirs. Scientific Reports, 11, Article 21730. https://doi.org/10.1038/s41598-021-01023-w

[39]. Suponik, T., Labus, K., & Morga, R. (2023). Assessment of the Suitability of Coke Material for Proppants in the Hydraulic Fracturing of Coals. Materials, 16(11), 4083. https://doi.org/10.3390/ma16114083

[40]. Tang, M., Ju, X., & Durlofsky, L. J. (2022). Deep-learning-based coupled flow-geomechanics surrogate model for CO2 sequestration. International Journal of Greenhouse Gas Control, 118, 103692. https://doi.org/10.1016/j.ijggc.2022.103692

[41]. Teufel, L. W., Rhett, D. W., & Farrell, H. E. (1991). Effect of reservoir depletion and pore pressure drawdown on in situ stress and deformation in the Ekofisk Field, North Sea. Proceedings of the 32nd U.S. Symposium on Rock Mechanics, ARMA-91-063. https://www.osti.gov/biblio/5807580

[42]. Tugan, M. F., & Weijermars, R. (2022). Searching for the root cause of shale well rate variance: Highly variable fracture treatment response. Journal of Petroleum Science and Engineering, 210, 109919. https://doi.org/10.1016/j.petrol.2021.109919

[43]. Wang, C., Wang, T., Jiang, T., Liu, J., & Zhu, Y. (2024). Proppant settlement and long-term conductivity calculation in complex fractures. ACS Omega, 9(11), 12547–12558. https://doi.org/10.1021/acsomega.3c08594

[44]. Weijermars, R. (2023). Production forecasting of unruly geoenergy extraction wells using Gaussian decline curve analysis. Geofluids, 2023, Article 5534305. https://doi.org/10.1155/2023/5534305

[45]. Weijermars, R., & Wang, J. (2021). Stress Reversals near Hydraulically Fractured Wells Explained with Linear Superposition Method (LSM). Energies, 14(11), 3256. https://doi.org/10.3390/en14113256

[46]. Xiao, C., Zhang, S., Ma, X., Zhou, T., & Li, X. (2022). Surrogate-assisted hydraulic fracture optimization workflow with applications for shale gas reservoir development: A comparative study of machine learning models. Natural Gas Industry B, 9, Article 100332. https://doi.org/10.1016/j.ngib.2022.03.004

[47]. Zhang, F., Huang, L., Yang, L., Dontsov, E., Weng, D., Liang, H., Yin, Z., & Tang, J. (2022). Numerical investigation on the effect of depletion-induced stress reorientation on infill well hydraulic fracture propagation. Petroleum Science, 19(1), 296–308. https://doi.org/10.1016/j.petsci.2021.09.014

[48]. Zhang, Y., Zuo, J., Fei, X., & Dong, S. (2024). Propagation Mechanism of Pressure Waves during Pulse Hydraulic Fracturing in Horizontal Wells. Applied Sciences, 14(16), 6982. https://doi.org/10.3390/app14166982

[49]. Zhao, J., Ren, L., Lin, C., Lin, R., Hu, D., Wu, J., Song, Y., Shen, C., Tang, D., & Jiang, H. (2025). A review of deep and ultra-deep shale gas fracturing in China: Status and directions. Renewable and Sustainable Energy Reviews, 209, Article 115111. https://doi.org/10.1016/j.rser.2024.115111